Theor. Appl. Climatol. (2004)
DOI 10.1007/s00704-004-0053-8

Theoretical and Applied Climatology
Printed in Austria

[1] University of Rome "La Sapienza", Department of Physics, Rome, Italy
[2] Meteorologisches Institut, Universität Hamburg, Hamburg, Germany
[3] Training Centre of China Meteorological Administration, Beijing, China

Spatio-temporal variability of dry and wet periods in eastern China

I. Bordi[1], **K. Fraedrich**[2], **J.-M. Jiang**[3], and **A. Sutera**[1]

With 5 Figures

Received July 18, 2003; revised January 3, 2004; accepted January 19, 2004
Published online September 3, 2004

Summary

An analysis, based on rain gauge observations, of the time-space variability of dry and wet periods during the last fifty years in eastern China is presented. The Standardized Precipitation Index (SPI) is used to assess the climatic conditions of the area, and principal component analysis (PCA) is applied to capture the pattern of co-variability of the index at different stations. Results suggest that the northern part of eastern China is experiencing dry conditions more frequently from the 1970s onwards indicated by a negative trend in the SPI time series. Long-term fluctuations characterize the SPI signal and contribute to the power spectrum variance at periods ranging from interdecadal to interannual time scales, that is respectively, 24 years and from 16 to 4–3.7 years. These periodic components provide a useful resource for long-term predictability of dry and wet periods in eastern China.

1. Introduction

Long term fluctuations of dry and wet conditions have been identified and monitored over continental watersheds in northern America which are affected by the North Pacific stormtrack, the El Nino-Southern Oscillation and other teleconnections (see, for example, Svoboda et al., 2002). Similarly, low frequency variability has been documented in central and southern Europe (for the Elbe river basin and Sicily, Bordi et al., 2004 and references therein), which is influenced by the tail end of the North Atlantic stormtrack. A surprising result from analysing wet and dry conditions in the Elbe basin and Sicily was that the low frequency variability in both areas showed strong similarity. To obtain a broader view of long term dry and wet period fluctuations, these regional analyses need to be extended to the watersheds of other regions. Here we present an analysis of eastern China with its exposure to highly complex atmospheric circulation regimes affected by monsoonal systems and mid-latitude disturbances, Siberia, and the Himalayan mountains.

Preceding studies of dry and wet periods in eastern China (Wang and Zhao, 1981; Clegg and Wigley, 1984; Jiang et al., 1997) describe the low frequency variability and abrupt changes during the last five hundred and thousand years, respectively, based on qualitative historical data. These studies are now extended and complemented by focussing on the last fifty years of instrumental precipitation records. These data are subject to an objective drought assessment (Bordi and Sutera, 2001, 2002), which is based on the standardized precipitation index (SPI, introduced by McKee et al., 1993, for an overview see Keyantash and Dracub, 2002). As the SPI characterizes water deficit and surplus, derived from precipitation alone, it can be easily computed. As the index is standardized, it is also suitable for comparing different regions or watersheds. Studies have demonstrated that the SPI is a useful tool to be established operationally as part of a drought monitoring system. Here we extend SPI monitoring in order to evaluate its potential for the prediction of dry and wet spells. Section 2 describes the data and the methods; Section 3 analyses the space-time variability of precipitation in the region, and an outlook for long-term predictability is provided in Section 4. Conclusions are presented in Section 5.

2. Data and methods of analysis

Periods of wet and dry condition can be characterized by an index which depends only on the monthly precipitation recorded at single stations. 160 stations in China, from 1951 to 2000, are chosen because of their record length and complete-

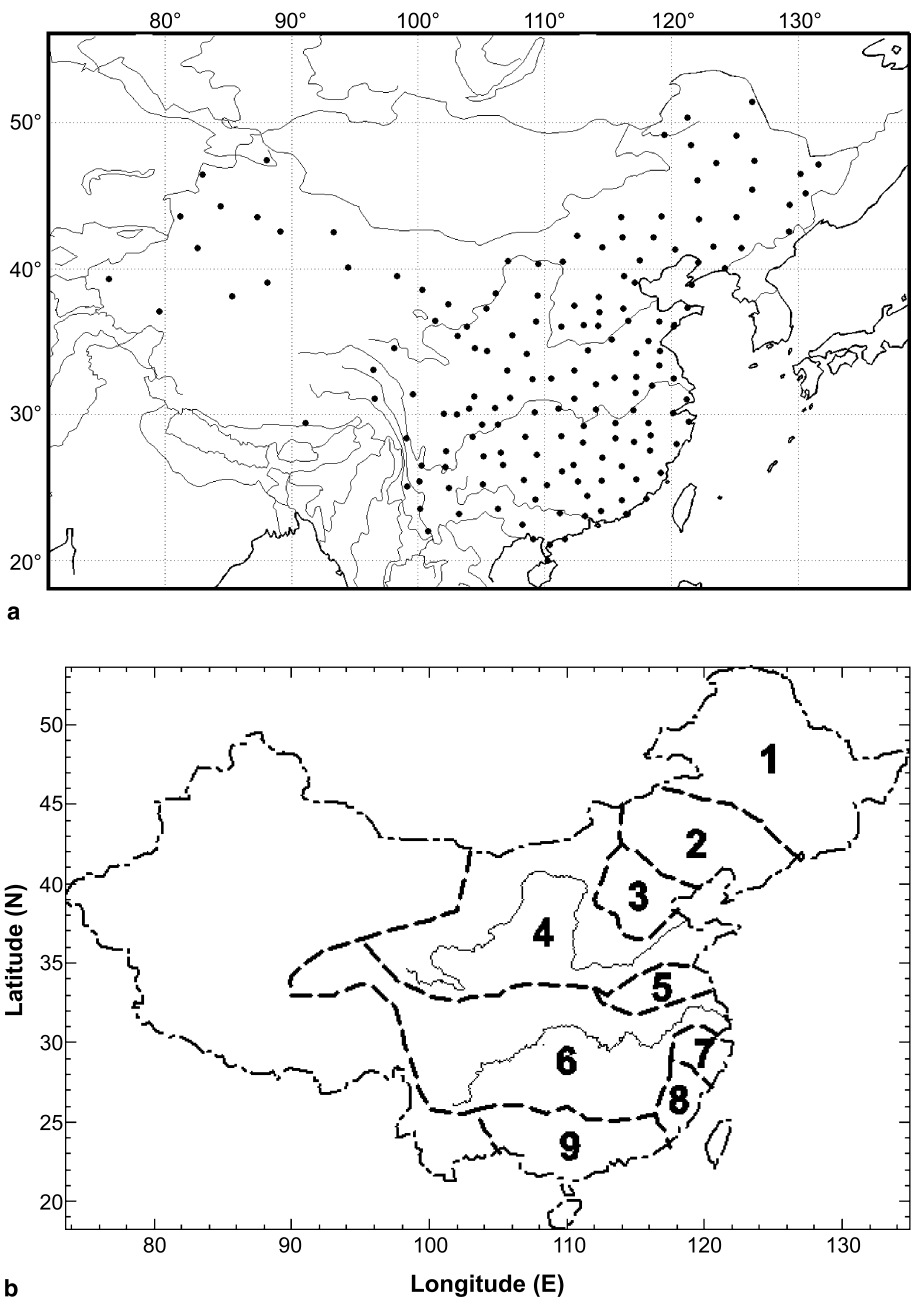

Fig. 1. Location of stations in China (**a**) and the nine watersheds (**b**)

ness, although we cannot exclude the occasional application of gap-filling routines (see Fig. 1a for their location). Because stations in the north-west and north-east are not homogeneously distributed in space, a restricted area of eastern China ($20° \mathrm{N} < \mathrm{lat} < 40° \mathrm{N}$, $100° \mathrm{E} < \mathrm{lon} < 120° \mathrm{E}$, with a total of 105 stations) has been considered. SPI-analysis is applied to the monthly mean precipitation time series of nine watersheds in central-eastern China (based on 16, 10, 7, 28, 7, 45, 5, 4, 14 stations, respectively). The location of the nine main river basins is shown in Fig. 1b. All time series are subject to the following analyses.

Standardized Precipitation Index (SPI): The Standardized Precipitation Index (SPI) is defined to describe dry and wet periods. It is based on time series of monthly precipitation cumulated over a period (or window-length ranging up to years). After fitting a Gamma distribution and transforming it to a normal distribution by an equal probability transformation, the SPI is computed as the precipitation anomaly of the transformed data, divided by the standard deviation of the transformed data (Guttman, 1999; Keyantash and Dracub, 2002; loc. cit.). The mapping into a normal distribution allows assessment of dry and wet periods of the same strength, which is defined by the same negative and positive thresholds of the symmetric normal distribution (see Bordi et al., 2004). Most importantly, the standardisation also enables comparison of different climatic or hydrological regimes, both in observations or numerical simulations. Since the SPI is computed for finite time-windows sliding over the precipitation time series, various kinds of droughts, such as meteorological, agricultural or hydrological, occurring on multiple time scales, may be monitored (Hayes et al., 1999). A window length of 24 months has

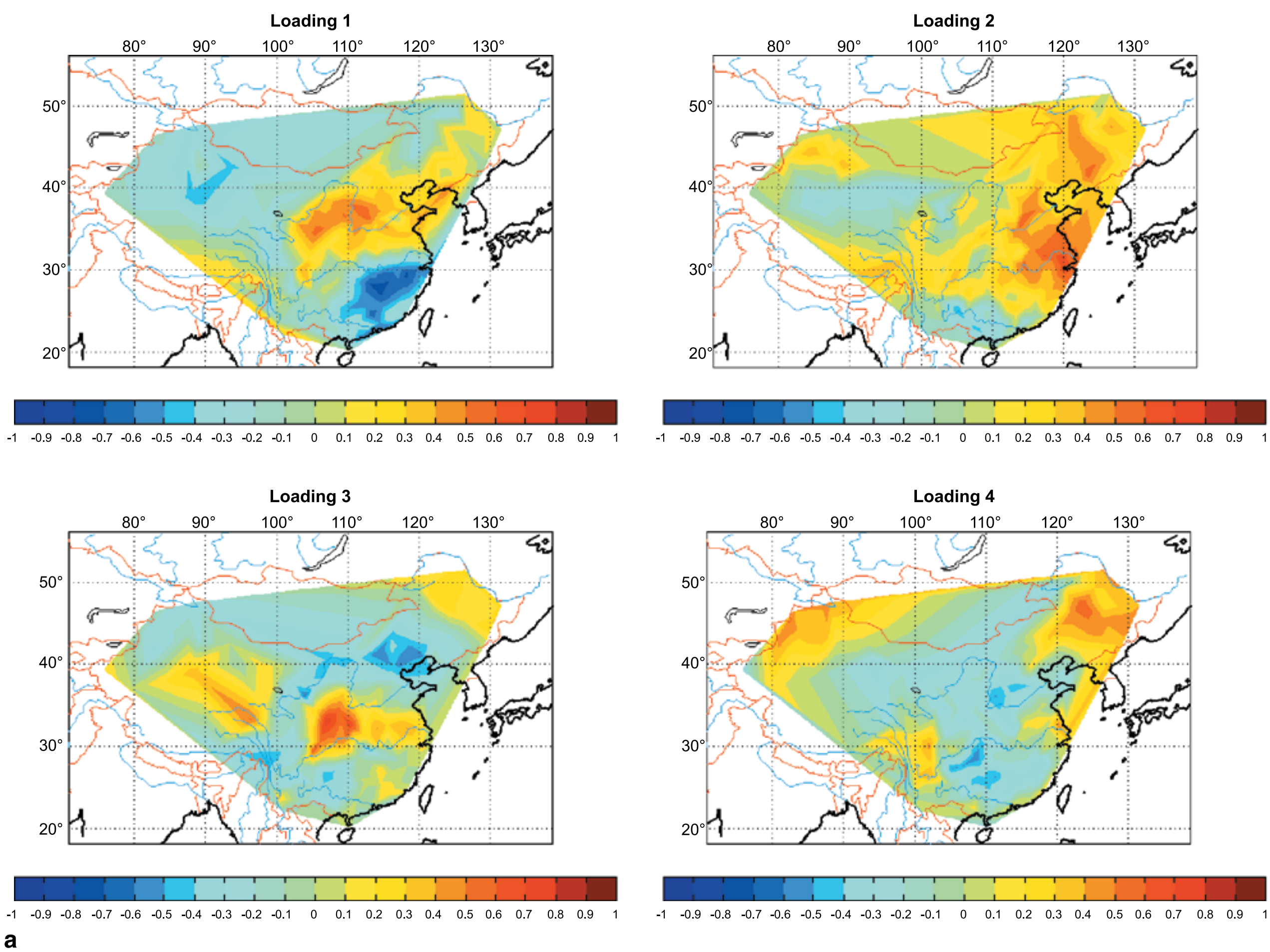

a

Fig. 2. First four loading patterns of the principal components of the SPI-24 in China (**a**) and eastern China (**b**). The percentage of the explained variance is shown in Table 1

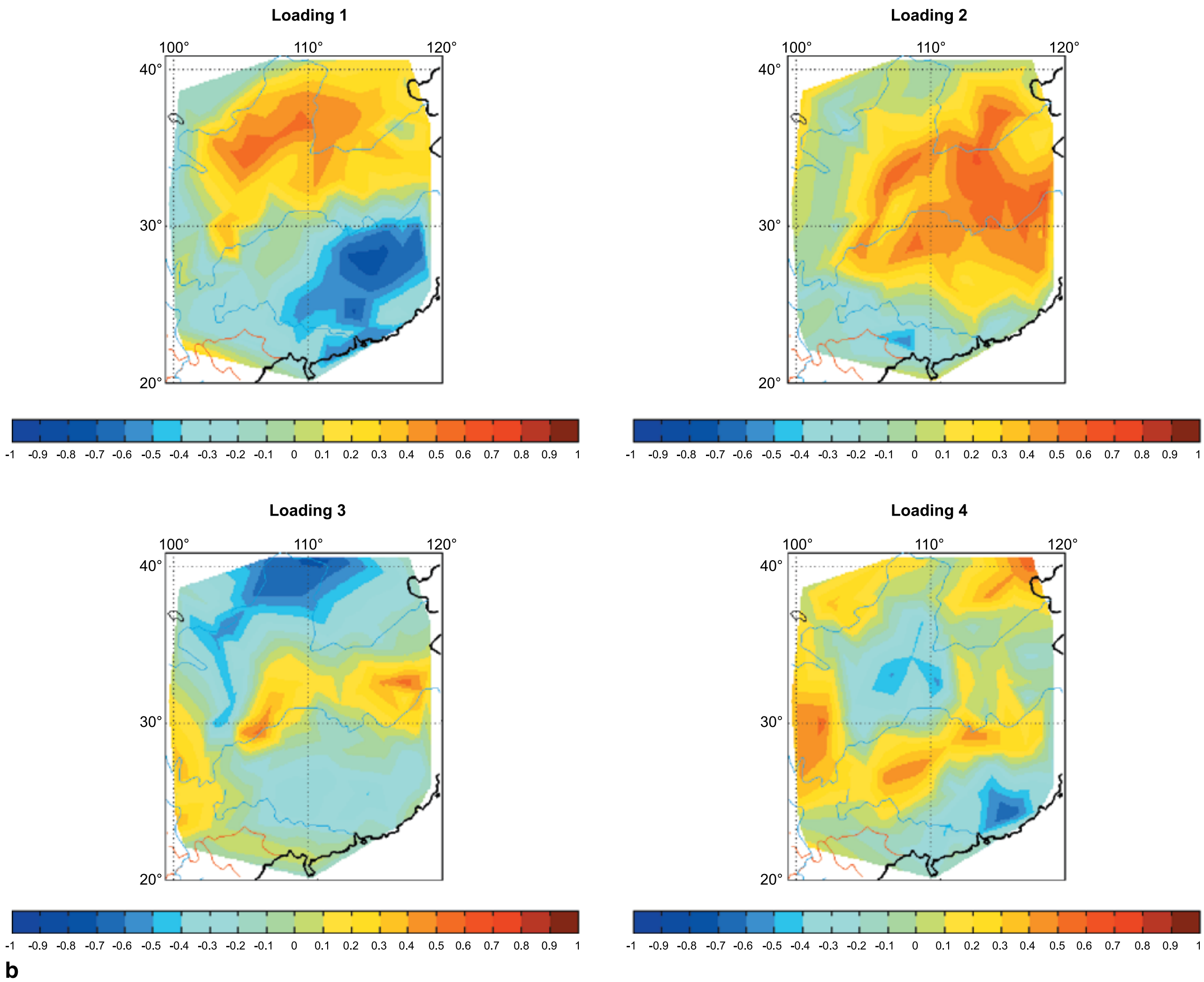

Fig. 2 (*continued*)

been proven as a suitable time scale (SPI-24, see Bordi et al., 2001), because it captures the low frequency variability, avoids an explicit annual cycle, and allows direct comparison with results from other studies (Bordi et al., 2004). According to the classification of the index values, a level crossing at SPI-24 $= \pm 2$ indicates transition to extreme wetness/dryness (see, for example, Bordi and Sutera, 2001), which corresponds to all values exceeding the 5% confidence interval.

Principal component analysis (PCA): To capture the patterns of covariability of SPI at different stations, we use PCA. This is basically a data reduction method, which generates a set of linearly independent spatial patterns (loadings). These display the spatial variability in terms of statistically deduced spatial modes and describe the correlation between SPI-series and the corresponding score (principal component or PC time series). Due to standardisation of SPI, the co-variability is represented by a correlation matrix. The spatial patterns are ordered with respect to their contribution to the total space-time variability (denoted in percent; for details see Rencher, 1998; Bordi and Sutera, 2001).

Power spectrum analysis: The scores are subject to power spectrum analysis (Jenkins and Watts, 1968) to identify their behaviour in the frequency domain with spectral peaks characterizing distinct frequency bands.

3. Results: Analysis and predictability

The first four loadings identified for the SPI-24 for the whole of China and eastern China are displayed in Fig. 2a and b, respectively, explain-

Table 1. Percentages of variance explained by the first four principal components for China, eastern China and the nine watersheds

N. PCs	% variance East China	% variance China	% variance 9 watersheds
1	14.2	11.2	29.8
2	11.1	9.2	27.8
3	8.9	7.7	12.1
4	7.6	7.5	10.9
Cumulative variance (%)	41.8	35.6	80.6

ing 35.6% and 41.8% of the total amount of cumulative variance (see Table 1). The following results are noted: (1) The first loading in Fig. 2a, which explains 11.2% of the total variance, shows a north–south dipole pattern in the eastern part of the domain with high positive/negative correlation with the corresponding PC score (see Fig. 3a). The corresponding first score (PC-1) is characterized by long-term oscillations superimposed on a negative trend from the 1970s onwards. This means that the areas identified by high positive values in the first loading have been affected by more frequent dry events during the more recent decades. (2) The second loading pattern (9.2%) is positive in the eastern part of the domain and the corresponding score reveals a residual trend component plus long-term periodicity; while the other loadings are very close in terms of variance explained, and their corresponding scores show several periodicities. (3) Similar annotations can be made for eastern

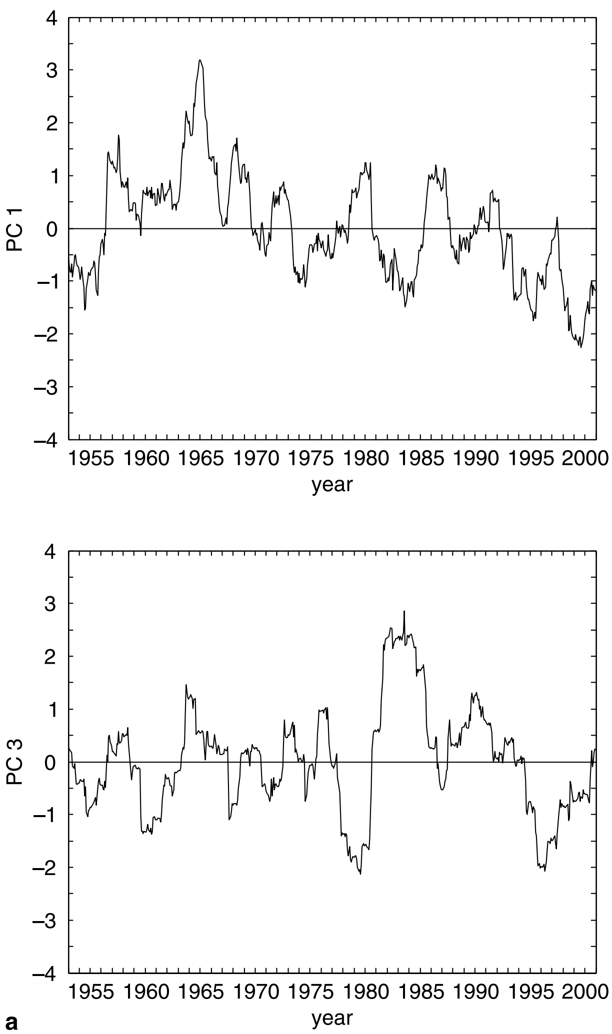

Fig. 3. First four scores of the loading patterns of the principal components of the SPI-24 in China (**a**), eastern China (**b**), and the nine watersheds (**c**)

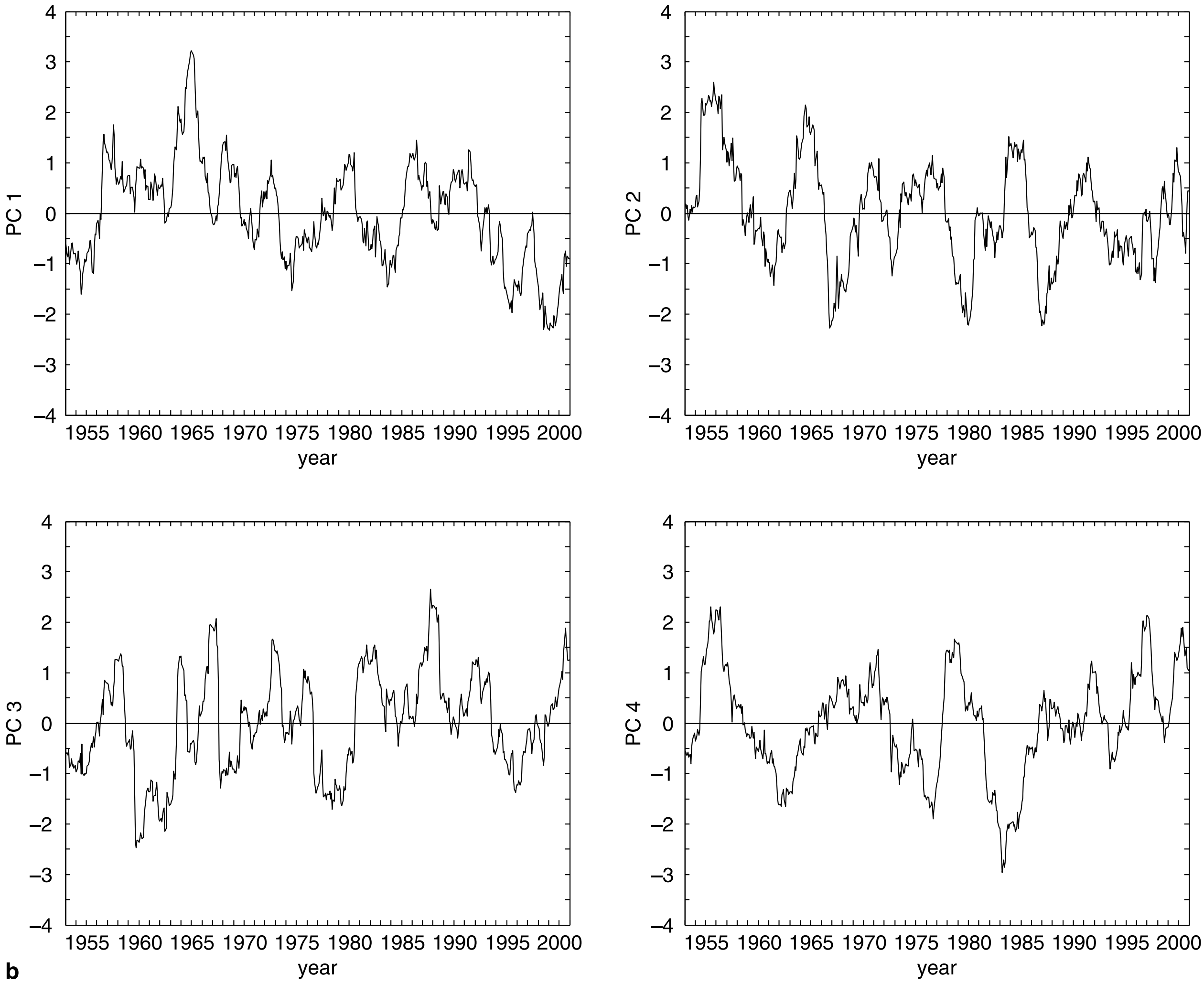

Fig. 3 (*continued*)

China (Fig. 3b). In fact, results for eastern China are very close to those obtained for China, especially for what concerns the first two loadings and principal component scores, even if the percentages of variance explained are little different. This result is not unexpected, given the loading pattern for the whole of China; it means that the poor spatial coverage of stations in western China hardly affects the analysis, so that we can focus on the eastern part.

River basins: The temporal variability revealed by the first PC score is associated with the variability of the nine watersheds: The order numbers from north to south are for the following river basins: (1) Heilongjiang, (2) Liaohe, (3) Haihe, (4) Huanghe (Yellow River), (5) Huaihe, (6) Changjiang (Yantze River), (7) Qiantangjiang, (8) Minjiang, and (9) Zhujiang. By computing the PCA of the SPI-24 for the nine river basins we obtain the following results:

1. The first four loadings explain about 80% of the total variance (see Tables 1 and 2).
2. The corresponding PC scores, shown in Fig. 3c, are very close to those obtained for the analysis of the whole of China SPI-24 (correlation coefficients are 0.84, 0.87, 0.59, 0.86).

The spatial covariability of the individual station time series is mainly reflected by the large-scale covariability of the watersheds. That is, the cumulative variance, 35.6%, explained by the first four loadings for the whole of China is mainly related to the 80.6% variance of the watersheds. An inspection of loading values reported in Table 2 suggests that basins 2–5 are highly correlated with the corresponding PC-1

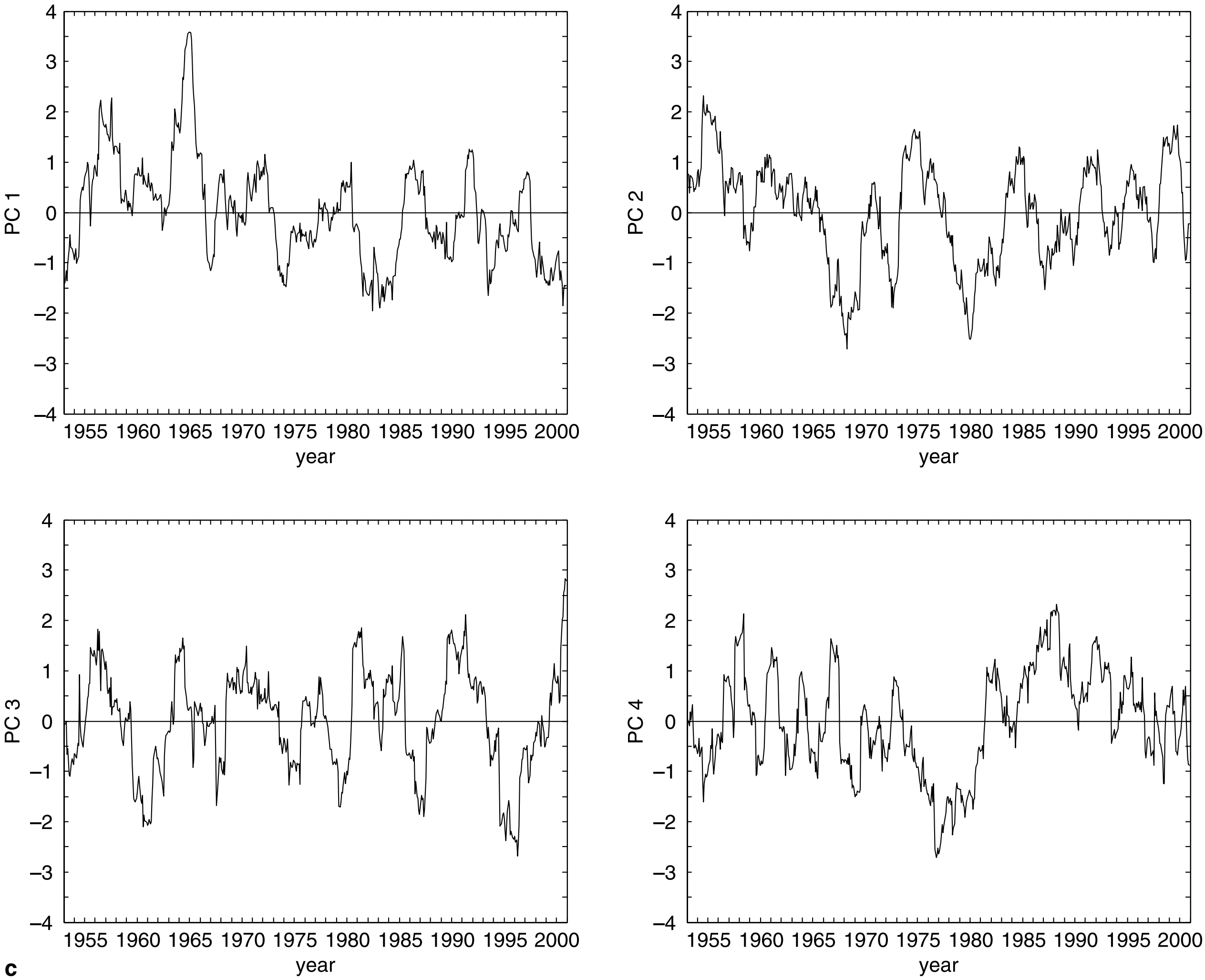

Fig. 3 (*continued*)

Table 2. First four loadings of the principal components of the SPI-24 for the nine watersheds. The percentage of the explained variance is shown in Table 1

N. river basins	Loading 1	Loading 2	Loading 3	Loading 4
1	.181	−.471	−.174	.810
2	.641	−.404	−.532	.073
3	.733	−.378	−.155	−.263
4	.701	−.267	−.096	−.398
5	.520	−.395	.499	.127
6	−.260	−.775	.369	−.187
7	−.462	−.800	.067	.014
8	−.507	−.698	−.104	−.142
9	−.631	−.142	−.582	−.156

(the negative trend characterizes these basins, in particular basin 3 and 4), basins 6–8 are highly correlated with PC-2, while basin 9 has negative correlation with PC-3 and basin 1 is highly correlated with PC-4. Topography and, in particular, the large scale meridional structure of the general circulation contribute to the spatial patterns, which are dominated by centres in the mid-latitudes and subtropics (loadings 1 and 2) and by the southern- and northern-most watersheds (loadings 3 and 4; see Table 2).

Power spectrum: The spectral analysis of PC-1 for eastern China is presented in Fig. 4. Considering the 95% confidence interval on a single spectral line, the following broad bands of spectral peaks are established as statistically significant. Each spectral band (of PC-1) consists of significant frequencies contributing to the statistically significant peaks (see Table 4). The following peaks characterize interdecadal, decadal, and interannual variability: A broad band peak is

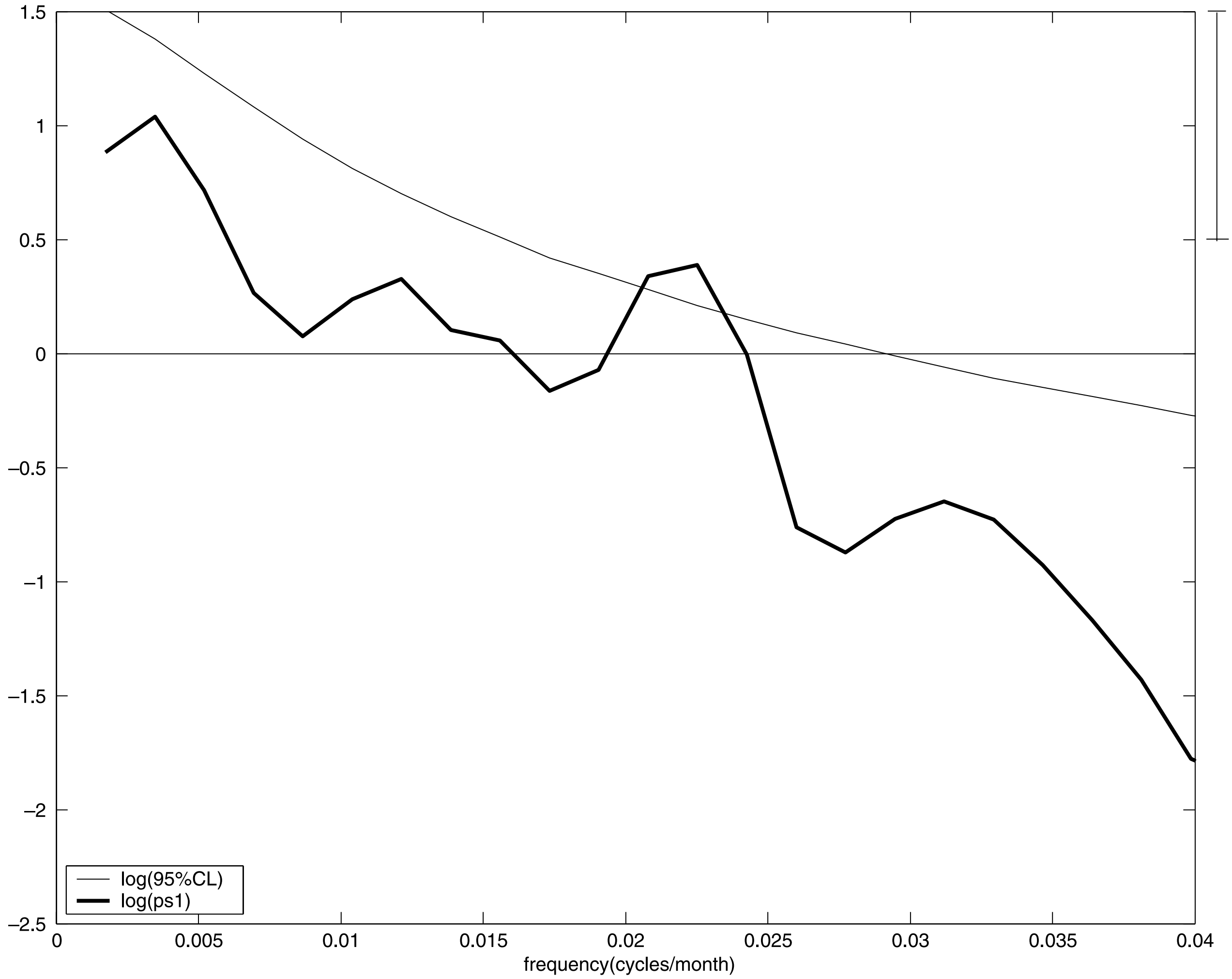

Fig. 4. Logarithm of the power spectrum for PC-1 of the SPI-24 for eastern China. The thin line is the first order autoregressive model adapted to the time series (with the same mean and variance). The vertical line is the 95% confidence interval

found centred around the interannual time scale, 4.0–3.7 years (see Table 3), suggesting a link with the El Niño/Southern Oscillation (ENSO) phenomenon. The other peaks lie near 6.9–8 up to 16 years and near 24 years, respectively. Here it must be pointed out that due to the short time series available the trend seems to be almost linear, but perhaps it is related to the long interdecadal periods detected around 24 and 48 years, although their statistical significance cannot be ascertained. Periodicities, similar to those shown in Table 4 for PC-1, have also been noted in the SPI computation for Europe based on NCEP/NCAR re-analysis data (Bordi and Sutera, 2001). They are also surprisingly close to those found for other regions analysed in some detail (Sicily and Elbe river basin, Bordi et al., 2004), even if they explain different percentages of spectral variance. To show the impact of these periodicities on dry and wet periods, we synthesise the PC-1 time series.

Table 3. Frequencies (cycles per month) and periods (in years) of the largest power for the statistically significant peaks determined for the score of the first principal component of eastern China

	Frequency (cycles/month)	Period (year)
PC-1: East China	0.00347	24.0
	0.01040–0.01213	8.0–6.9
	0.02080–0.02253	4.0–3.7

Time series reconstruction: The PC-1 time series (up to November 2000) is synthesised by

Table 4. Periods retained for reconstructing the time series associated with the first principal component (PC-1) for eastern China and the SPI-24 for station n.88. The power spectrum variance explained by each periodicity is also listed

Channel	PC-1 East China		Station n. 88 East China	
	Period (year)	Variance (%)	Period (year)	Variance (%)
1	48.1	15.1	48.1	10.2
2	24.0	36.5	24.0	27.4
3	16.0	2.9	16.0	2.6
4	12.0	5.9	12.0	8.3
6	8.0	3.8	8.0	17.3
7	6.9	6.8	–	–
9	5.3	4.2	5.3	2.3
10	–	–	4.8	2.9
11	–	–	4.4	7.2
12	4.0	5.3	–	–
13	3.7	7.3	–	–
17	–	–	2.8	2.9
Cumulative variance (%)		87.8		81.1

filtering out all the frequencies except those listed in Table 4. Each band consists of all significant frequencies, which contribute to the statistically significant peaks. The criterion for selecting periods to be considered for the reconstruction consists of retaining those that explain at least 2% of the power spectrum variance. As shown in Table 4, the most relevant frequencies explain more than 6% of variance. Altogether, they explain 87.8% of the PC-1 fluctuations, which describe 14.2% of the eastern China spatio-temporal SPI variability (Tables 1, 3). Similar frequency bands have been noted in the SPI computation for Italy and Europe (see Table 3 in Bordi et al., 2004). A comparison of the eastern China PC-1 temporal behaviour and the corresponding re-synthesised time series is shown in Fig. 5a. Not unexpectedly, the main dry and wet periods of the region are essentially represented by the dominating periods. At first sight, this can be inferred from the low frequency variability presented in Fig. 2a and Table 3 (long term trend and decadal variability). This analysis indicates a high potential predictability both by statistical and/or dynamical methods. However, the latter method would require a physical explanation in terms of the underlying processes. So far we have not found any conclusive mechanism for the source of these periodicities, though some frequencies involved suggest a relationship with ENSO.

Single station: Here we demonstrate that the behaviour identified for PC-1 can also be found at a single station. The SPI-24 time series of station n.88 (34.35° N, 105.45° E) is highly correlated (0.6) with the PC-1. Its power spectrum (not shown) has statistically significant periodicities at roughly the same sequence of frequencies as obtained for PC-1. In Fig. 5b we show the SPI-24 at this station and the relevant periodic components as listed in Table 4. Note that, for this station, the retained periodic components explain a large amount of the station's total climatic variability, with some variance which appears to be related to the unfiltered long-term trend.

Potential predictability of dry and wet periods: The SPI has so far been utilised to monitor dry and wet periods. To forecast the future evolution of dry or wet periods, however, requires suitable model building and physical insight into the underlying atmospheric processes. Statistical methods may lead to skillful local or global models in a n-dimensional space, spanned by a sufficiently large number of independent PCs of the SPI. Such phase space predictions may be extended by including parameters or indices which characterize the larger scale climate system linked to the dominating period bands. Since dryness and wetness seem to be driven by the periodicities outlined above, a simple method to assess potential predictability of the occurrence of these climatic phenomena may be based on the forward extrapolation of the detected periodic components. As an example we use only PC-1 for eastern China and SPI-24 for the station n.88. The data set is updated to December 2002 and the monthly "forecasts" are made from December 2000 to December 2002. They are computed by forward extrapolation of the periodic signals, which have been estimated up to November 2000. Two prediction sets are obtained, one for PC-1 and the other for station n.88; each set consists of one extrapolation per lead time step, which increases from one month to two years. The mean values of departures of extrapolations from observations with their standard deviations, for PC-1 and the SPI-24 of station n.88, are (0.13 ± 0.10) and (0.21 ± 0.06) respectively. It must be noted that the single station SPI-24 extrapolation is systematically higher in its underestimate of dryness.

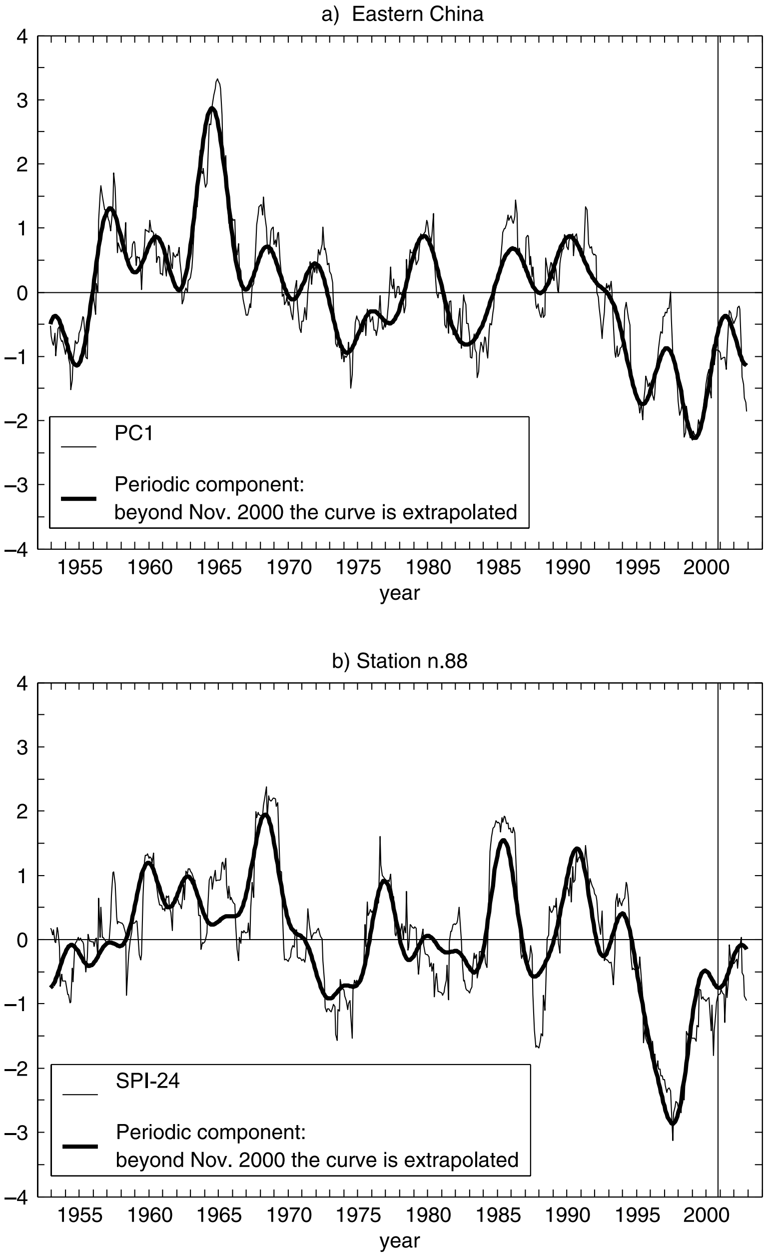

Fig. 5. Observed (thin line) and reconstructed (thick line) time series: The reconstruction (up to November 2000) is based on the significant spectral frequencies of the score of the first principal component, PC-1, of the SPI-24 for eastern China (**a**), and the single station n.88 (**b**), whose SPI is highly correlated (0.6) to PC-1. Periods considered are listed in Table 4. Note that from December 2000 to December 2002 the time series reconstruction is extrapolated

In general, the method produces good results, keeping in mind that it is only a predictability of the envelop of the index (that is, its first PC) that is expected, which leaves the higher frequency fluctuations unresolved.

4. Conclusions

Many studies have examined long time series of precipitation data (of the warm season or the annual mean) for eastern China (for example Wang and Zhao, 1981; Clegg and Wigley, 1984; Qi and Feng, 2001). These studies revealed multi-decadal to centennial variations in the area, while an analysis of the spatial structure of these variations shows that when a dry situation was observed in southern China a wet situation was found in the eastern part and vice versa. The analysis proposed here extends and complements these studies: we focus on the last fifty years of observed precipitation records, applying the SPI for an objective drought assessment. This index allows comparison of different regions and monitors dry and wet periods that occur on different time scales. Results for long-term climate variability show a general agreement with those of the previous studies: since the 1970s the northern part of eastern China has experienced drought events more frequently evidenced by the presence of a negative trend in the SPI series. This is perhaps related to interdecadal periodicities in the SPI signals which, however, cannot be ascertained given the short time series available. Other interannual and decadal periods contribute to the power spectrum variance spanning from 3 to 16 and 24 years. Similar frequencies have also been revealed in the SPI analysis for Europe with NCEP/NCAR data and for the Sicily-Elbe regions with rain gauges observations. Furthermore, results follow those obtained with the same method of analysis for various regions of the Northern Hemisphere using the NCEP/NCAR re-analysis data set (see first loading and score, Bordi and Sutera, 2001; Panel XV–XVI), suggesting consistency between the re-analysis precipitation records in China and the rain gauge observations. The reconstruction of the SPI time series with periodicities, which greatly contribute to the total power spectrum variance, reveals good results and provides good possibilities for long term prediction of dry and wet periods by using detailed forecast methods (not developed yet). Floods, however, which are embedded in these processes, need further consideration, because their time scale is much shorter than that the dry and wet periods analysed here. Further efforts will be devoted to this and to analysis of the relation between low frequency fluctuations of sea surface temperatures (Fraedrich and Blender, 2003) and dry/wet periods on other continents.

Acknowledgements

Bordi and Sutera acknowledge the financial supports provided by CNR (grant "Accordo di Programma MURST-CNR Ecosistemi Marini") and ASI (grants CLOUDS, GEO-MED, CASSINI and GOMAS). Referees' comments are appreciated.

References

Bordi I, Sutera A (2001) Fifty years of precipitation: some spatially remote teleconnections. Water Res Manage 15: 247–280

Bordi I, Frigio S, Parenti P, Speranza A, Sutera A (2001) The analysis of the standardizes precipitation index in the mediterranean area: Large scale patterns. Annali di Geofisica 44: 965–978

Bordi I, Sutera A (2002) An analysis of drought in Italy in the last fifty years. Il Nuovo Cimento 25C: 185–206

Bordi I, Fraedrich K, Gerstengarbe F-W, Werner PC, Sutera A (2004) Potential predictability of dry and wet periods: Sicily and Elbe-Basin (Germany). Theor Appl Climatol (in press)

Clegg SL, Wigley TML (1984) Periodicities in precipitation in north-east China, 1470–1979. Geophys Res Lett 11: 1219–1222

Fraedrich K, Blender R (2003) Scaling of atmosphere and ocean temperature correlations in observations and climate models. Phys Rev Lett 90: 108501-(1–4)

Guttman NB (1999) Accepting the Standardized Precipitation Index: a calculation algorithm. J Amer Water Resour Assoc 35: 311–322

Hayes MJ, Svoboda MD, Wilhite DA, Vanyarkho OV (1999) Monitoring the 1996 drought using the standardized precipitation index. Bull Amer Meteor Soc 80: 429–438

Jiang J, Zang D, Fraedrich K (1997) Historic climate variability of wetness in East China (960–1992) A wavelet analysis. Int J Climatol 17: 969–981

Jenkins GM, Watts DG (1968) Spectral analysis and its applications. Holden-Day, Inc., 500 Sansome Street, San Francisco, California, 525 pp

Keyantash J, Dracup JA (2002) The quantification of drought: an evaluation of drought indices. Bull Amer Meteor Soc 83: 1167–1180

McKee TB, Doesken NJ, Kleist J (1993) The relationship of drought frequency and duration to time scales. Preprints, 8th Conference on Applied Climatology, 17–22 January, Anaheim, CA, Amer Meteor Soc 179–184

Qi H, Feng S (2001) A southward migration of centennial-scale variations of drought/flood in eastern China and the western United States. J Climate 14: 1323–1328

Rencher AC (1998) Multivariate statistical inference and applications. John Wiley & Sons, 559 pp

Svoboda M, LeComte D, Hayes M, Heim R, Gleason K, Angel J, Rippey B, Tinker R, Palecki M, Stooksbury D, Miskus D, Stephens S (2002) The drought monitor. Bull Amer Meteor Soc 83: 1181–1190

Wang SW, Zhao ZC (1981) Droughts and floods in China, 1470–1979. In: Wigley TML, Ingrasham MJ, Farmer G (eds) Climate and history. Cambridge University Press, pp 171–288

Authors' addresses: Isabella Bordi (e-mail: bordi@romatm9.phys.uniroma1.it) and Alfonso Sutera, University of Rome "La Sapienza", Department of Physics, I-00185 Rome, Italy; Klaus Fraedrich, Meteorologisches Institut, Universität Hamburg, D-20146 Hamburg, Germany; Jian-Min Jiang, Training Centre of China Meteorological Adminstration, Beijing, 100081, China.